THE GREAT WORLD OF NANOTECHNOLOGY

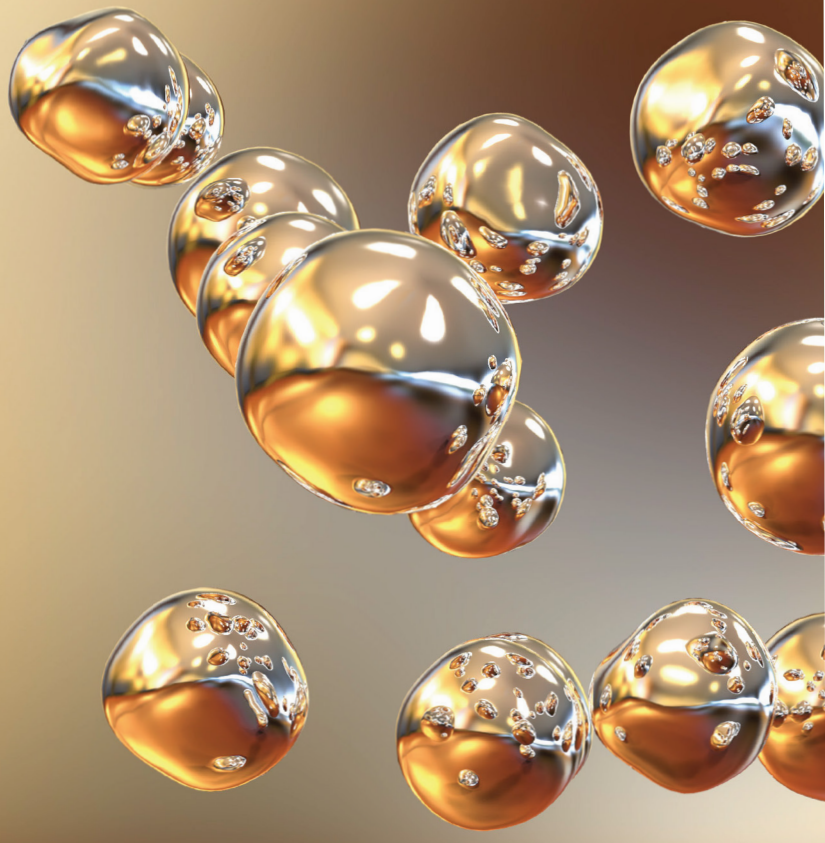

Marcos Augusto de Lima Nobre

(Organizador)

VOL II

EDITORA ARTEMIS
2021

THE GREAT WORLD OF NANOTECHNOLOGY

Marcos Augusto de Lima Nobre

(Organizador)

VOL II

EDITORA ARTEMIS
2021

Editora Chefe Profª Drª Antonella Carvalho de Oliveira
Editora Executiva M.ª Viviane Carvalho Mocellin
Direção de Arte M.ª Bruna Bejarano
Diagramação Elisangela Abreu
Organizadoras Prof. Dr. Marcos Augusto de Lima Nobre
Imagem da Capa Kateryna Kon
Bibliotecário Maurício Amormino Júnior – CRB6/2422

Editora Artemis
Curitiba-PR Brasil
www.editoraartemis.com.br
e-mail:publicar@editoraartemis.com.br

Dados Internacionais de Catalogação na Publicação (CIP)
(eDOC BRASIL, Belo Horizonte/MG)

G786 The great world of nanotechnology [livro eletrônico] : vol. II /
Organizador Marcos Augusto de Lima Nobre. – Curitiba, PR: Artemis, 2021.

Formato: PDF
Requisitos de sistema: Adobe Acrobat Reader
Modo de acesso: World Wide Web
Inclui bibliografia
Edição bilíngue
ISBN 978-65-87396-36-1
DOI 10.37572/EdArt_300621361

1. Nanociência. 2. Nanotecnologia. I. Nobre, Marcos Augusto Lima.

CDD 620.5

Elaborado por Maurício Amormino Júnior – CRB6/2422

EDITORA ARTEMIS
2021

Editora Artemis
Curitiba-PR Brasil
www.editoraartemis.com.br
e-mail:publicar@editoraartemis.com.br

PREFACE

The insertion of new and enhanced materials based on materials belonging to the Nano scale in the day-by-day has growth up in a silent way. In part, a number of works in the nanotechnology stemming of theoretical research using Density Functional Theory (DFT) and sophisticated simulation methods; another part is associated to the protected technologies associated to the military and patented nanomaterial and its process. In this sense, open access to recent aspects on the nanostructures application and properties can be reached in this book. Here, an interesting set of chapters gives opportunity of access texts that reach process and processing of nanostructures, applications of nanotechnology, advanced techniques to theoretical development. A broad set of nanostructures are here covered such as, nanocrystal, superficial nanograins, inner microstructures with nanograins, nanoaggregates, nanoshells, nanotubes, nanoflowers, nanoroad, nanosheets, Also, reveals new investigations areas as grainboundary of nanograins in ceramics and metals. A great number of software has been used as a tool of development of Science and Technologies for nanotechnology COMSOL Multiphysics 5.2. Phenomena and properties has been investigated by recent or classical techniques of materials characterization as Localized Surface Plasmon Resonance (LSPR), X-ray photoelectron spectroscopy (XPS), Field Emission Gun Scanning Electron Microscopy (FEG-SEM) with Energy Dispersive Spectroscopy (EDS), Raman Scattering Spectroscopy (RSS), X ray diffraction (XRD), ^{57}Fe Mössbauer spectroscopy, UV-vis spectroscopy, dynamic light scattering (DLS), Atomic Force Microscopy (AFM), and Field Emission Gun Scanning Electron Microscopy (FEG-SEM). In this sense, collections of spectra from Mössbauer spectroscopy, UV-vis spectroscopy and Infrared spectroscopy can be found. As a matter of fact, some chapter's item can be seemed as specific protocols for synthesis, preparations and measurements in the nanotechnology.

I hope you enjoy your reading.

Prof. Dr. Marcos Augusto Lima Nobre

TABLE OF CONTENTS

CHAPTER 7

FORMATION OF METAL NANOPARTICLES BY SPUTTER DEPOSITION ON UNCD FILMS BY NPIII INSIDE CONDUCTIVE TUBES

Data de submissão: 29/03/2021
Data de aceite: 16/04/2021

Nazir Monteiro dos Santos
National Institute for Space Research
Associated Laboratory of Plasma
São José dos Campos, SP, Brazil
nazirmonteiro@gmail.com
https://orcid.org/0000-0002-1518-9403

Divani Carvalho Barbosa
Faculty of Technology of Taubaté
State Center for Technological Education
Paula Souza
Taubaté, SP, Brazil
divanibarbosa@gmail.com
https://orcid.org/0000-0003-4938-4095

Evaldo José Corat
National Institute for Space Research
Associated Laboratory of
Materials and Sensors
São José dos Campos, SP, Brazil
evaldo.corat@inpe.br
https://orcid.org/0000-0003-3011-5522

Mario Ueda
National Institute for Space Research
Associated Laboratory of Plasma
São José dos Campos, SP, Brazil
mario.ueda@inpe.br
http://lattes.cnpq.br/9226460532838417

ABSTRACT: Surface modification of ultrananocrystalline diamond (UNCD) films by Nitrogen Plasma Immersion Ion Implantation (NPIII) using conductive tubes was studied. UNCD films were deposited on titanium substrates by CVD process using a hot filament reactor. The UNCD films were treated by NPIII inside stainless steel metallic tubes. The tubes, with 150 mm of length and different diameters, containing the UNCD films were placed in the interior of vacuum chamber of 600 liters. Field Emission Gun Scanning Electron Microscopy (FEG-SEM) with Energy Dispersive Spectroscopy (EDS) auxiliary, X-Ray Diffraction (XRD), Raman Scattering Spectroscopy (RSS), and X-ray Photoelectron Spectroscopy (XPS) were used to investigate the effect of NPIII treatment on UNCD films. The results showed that the NPIII treatment changed the surface morphology of UNCD films, increased the degree of disorder and the structural defects, and the formation of metallic nanoparticles by sputter deposition of the materials from the conductive tubes. Surface analysis have also demonstrated substantial dependence of NPIII with the conductive tubes diameter. For the UNCD film treatment by NPIII inside tube with diameter of 110 mm (T110), there was formation of metal oxide and nitride layers on the surface. For the treatment carried out inside the tube with a diameter of 40 mm (T40), there was implantation of metallic particles, indicating that the surface of the UNCD films was completely covered by iron (Fe°).

KEYWORDS: Plasma Immersion Ion Implantation. Surface Modification. Ultrananocrystalline Diamond Films. Conductive tubes.

1 INTRODUCTION

Plasma immersion ion implantation (PIII) is a well-known technique used for the three-dimensional surface modification of materials by ion implantation [1]. Recently, new developments in PIII using conductive tubes have been attained [2]. Both moderate (< 450 °C) and high temperature (> 700 °C), PIII inside tubes are now possible. Tube temperature is dependent on the diameter when hollow cathode plasma is produced inside it for PIII treatments of the tube walls, components or samples. Hollow cathodes are also providing plasmas for materials surface modifications [3], in particular, using PIII method in tubular or concave geometry samples or workpieces [4]. UNCD films have been the subject of large interest in the scientific community, motivated by their exceptional properties for tribological [5], mechanical [6, 7], biomedical [8] and electronic [9] applications. This interest is especially due to their high smoothness, electron field emissity [10], as well as their unique capability to incorporate n-type dopants [11, 12]. Nitrogen atoms, adsorbed in diamond, upon equilibration at elevated temperatures tend to enrich at the surface and at grain boundaries. Adsorbed nitrogen atoms on UNCD surfaces strongly affect their physico-chemical properties and phenomena as surface energy, morphology, equilibrium shape, surface diffusion and sintering, adhesion and wear, surface reactivity and corrosion, metal-gas reactions and catalytic reactions [13]. In addition, adsorption at grain boundaries strongly influences materials properties, and the adsorbed nitrogen atoms are of special interest as effective semiconductor. Nitrogen incorporation in the UNCD structure is recognized to affect most of the film properties, including changes in the tribological behavior, molecular structure and chemical bonds. Nitrogen incorporation results in the enhanced adhesion strength of UNCD films by increasing sp^2 bonds and subsequently relaxing residual stress in the films [14]. In addition, the tribological performance of UNCD films can be improved by nitrogen incorporation because promotes the graphitization of the films and could be used in protective and coating technologies.

In this study, we have been exploring NPIII treatment using different size stainless steel (SS)304 tubes with diameters of 110 mm (T110) and 40 mm (T40) with length of 150 mm for the surface modification of UNCD film. PIII is a powerful tool for adding impurities to a host material. We attempt to elucidate the effects of NPIII treatment on the structural, morphological, and chemical properties of UNCD films. The results shows that the structure of UNCD film surface was modified by NPIII treatments and metallic nanoparticles were implanted by sputter deposition. This treatment can certainly include

other species that would give UNCD films with other properties and applications including enhanced magnetic UNCD.

2 EXPERIMENTAL

2.1 SUBSTRATE PRETREATMENT

To improve the adhesion of the diamond film on the titanium substrate and the nucleation density during growth of the films, we performed a pre-treatment on the surface of substrates, which consists of a mechanical incision by blasting with glass beads, whose main objective is to increase roughness [15]. After this, the substrates (15 mm x 15 mm x 1 mm) were cleaned with acetone in an ultrasonic bath in order to remove grease or any other contaminants. Soon after, the substrates were prepared for growth by plating with nanometric diamond powder in ultrasonic hexane bath during 60 minutes to enhance diamond nucleation.

2.2 UNCD FILMS PRODUCTION

Ultrananocrystalline diamond (UNCD) films were produced on titanium substrate using Hot Filament Chemical Vapor Deposition (HFCVD) technique. The films were carried out using an experimental system from the Associated Laboratory of Sensors and Materials/Group of Diamond and Related Materials at National Institute for Space Research. The experimental setup is composed of the reactor made of a stainless steel cylindrical shape chamber with Pyrex windows and copper coil through which cooling water circulates. The internal layout of the reactor consists of five filament of tungsten with diameter of 125 μm supported by two brackets of molybdenum and a gas inlet tube located just above the region of the filaments. The distance between the filaments and the substrate was 5 mm and the deposition time was 7 h. The chemical process included treatments in CH_4/H_2/Ar gases with 9 vol.% hydrogen, 1 vol.% methane and 90 vol.% argon at a total flow of 200 sccm (standard centimeter cubic per second). The temperature and the pressure inside the reactor were maintained at 750 °C and 30 Torr, respectively. Details of deposition set-up and procedure have been described earlier [16]

2.3 UNCD FILMS TREATMENT BY NPIII INSIDE CONDUCTIVE TUBES

UNCD films were treated during 120 min by nitrogen plasma immersion ion implantation (NPIII) inside conductive tubes, with 150 mm in length and different diameters. The NPIII treatments employed here was carried out using an experimental system from

the Associated Laboratory of Plasma at National Institute for Space Research. It consists of a cylindrical vacuum chamber of 600 liters with a vacuum system composed of a mechanical, a root and a diffusion pumps. Its detailed description is found in some recent published paper of our research group [17], with a difference that the SS pipes were connected directly to the high voltage pulser and no additional plasma source was used. Stainless steel (SS) tubes were placed in the interior of cylindrical vacuum chamber and were isolated from the ground by a set of dielectric insulators (corrugated alumina tubes, then a glass plate, and a Makor support and alumina tubings), as can be seen in Fig.1 (a) and 1(b). In this set-up, samples of UNCD films fixed to the inside wall of the tube were bombarded with accelerated nitrogen ions. The temperature distribution at the end of the treatment was measured with an infrared pyrometer (Mikron, model MK-90Q), looking at the middle positions of the tubes. The NPIII treatment conditions are shown in Table 1.

Fig. 1. Stainless steel tubes with diameters of (a) 110 mm (T110) and (b) 40 mm (T40) that were used to perform NPIII treatments on UNCD films surface.

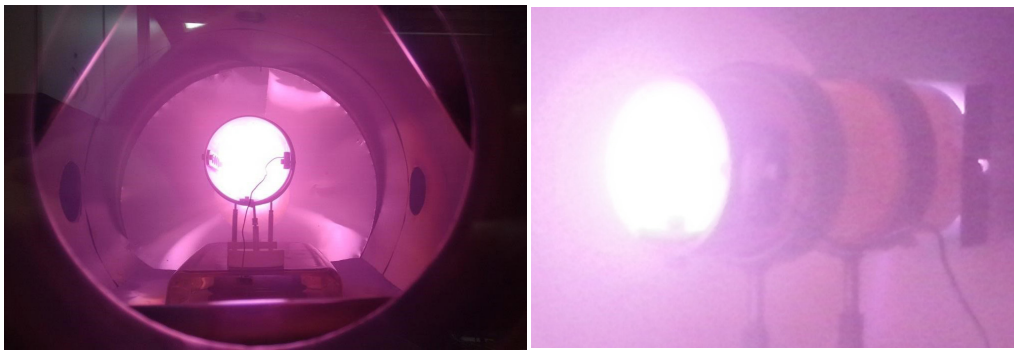

(a) Pulser - on (b) Pulser - on

As can be seen from Table I, the nitrogen pressure used in T110 was about 3.0 Pa. The pulser was operated at pulse length of 30μs and at a frequency of 1 kHz. Using peak voltages of 3 kV and peak currents of 3 A, the implantation condition led to the tube temperature in the order of 380°C, in this case of SS304 tube with 110 mm Ø and both sides of the tube open (Fig. 1(a)).

Table I. Conditions of NPIII treatments on UNCD films surface inside T110 and T40 size conductive tubes.

NPIII	Tube Diameter Size (mm)	Peak Pulse Current (A)	Peak Pulse Voltage (kV)	Frequency (kHz)	Final Temperature (°C)	Argon Time (min)	Pulse Length (μs)	Pressure of Nitrogen (Pa)
T110	110	3.0	3.0	1.0	380	10	30	3.0
T40	40	2.0	2.7	3.0	780	10	30	3.0

In case T40, a 40 mm Ø SS304 tube was closed in one end, using a thin sheet of SS304, as can be seen in Fig.1 (b). This resulted supposedly in much higher density plasma inside the tube. The operation condition was now: nitrogen pressure of 3.0 Pa, pulse length of 30 μs, at a frequency of 3 kHz, reaching peak voltage of 2.7 kV and peak pulse current of 2.0 A. The resultant plasma showed much higher light emission and soon after turning on the pulser, the tube started glowing due to the very high temperatures reached there.

2.4 SURFACE CHARACTERIZATION SYSTEMS

The analysis of crystallinity was performed by X-Ray Diffraction (XRD) in a Philips 3410 diffractometer in the Seeman-Bolin 2θ scanning mode using Cu Kα radiation (λ=0.154056nm). The evaluations of the morphology and the content of various elements in the UNCD films were investigated before and after the NPIII treatment, using Field Emission Gun Scanning Electron Microscopy (FEG-SEM) – Hitachi microscope model SU-70 (Tescan MIRA3) with auxiliary Energy Dispersive Spectroscopy (EDS) at an operating voltage of 25 kV. The quality of UNCD films and the existence of carbon layer was evaluated by Raman Scattering Spectroscopy (RSS) – Labram HR evolution – Horiba Scientific with a 514 nm excitation light source by argon ion laser. The chemical bonding states of the UNCD films before and after NPIII treatment were analyzed using X-ray Photoelectron Spectroscopy (XPS) - Thermos Scientific K-Alpha with monochromatic Al-Kα radiation (1486.6 eV). The binding energies in the spectra were calibrated with carbon (C1s 284.8 eV) peak. Instrument base pressure was about 10^{-10} Torr and high-resolution spectra were collected with 40 eV pass energy. The surface samples were sputter cleaned prior to analysis using a 4 kV argon ion beam by 1200 seconds. Spectra were analyzed using casaXPS software (version 2.3.15). Gaussian (30%)-Lorentzian (70%), defined in CasaXPS as GL (30), profiles were used for each component and a standard Shirley background are used for all reference samples spectra.

3 RESULTS AND DISCUSSION

3.1 STRUCTURAL SAMPLES CHARATERIZATION

X-ray diffraction (XRD) analysis was carried out to investigate the structural properties of titanium substrate, and UNCD films, before and after NPIII treatments, in T110 and T40 tubes, and the results are shown in Fig. 2. It can be observed that the Ti substrate have α-phase – hexagonal close-packed (hcp) crystalline structure. The 35°,

38°, 40.1°, and 52.8°, diffraction peaks can be observed relative to the titanium diffraction planes (100), (002), (101), (102), respectively (JCPDS 89-5009) [18].

Fig. 2. XRD pattern of Ti substrate, UNCD film before and after NPIII treatment in T110 and T40.

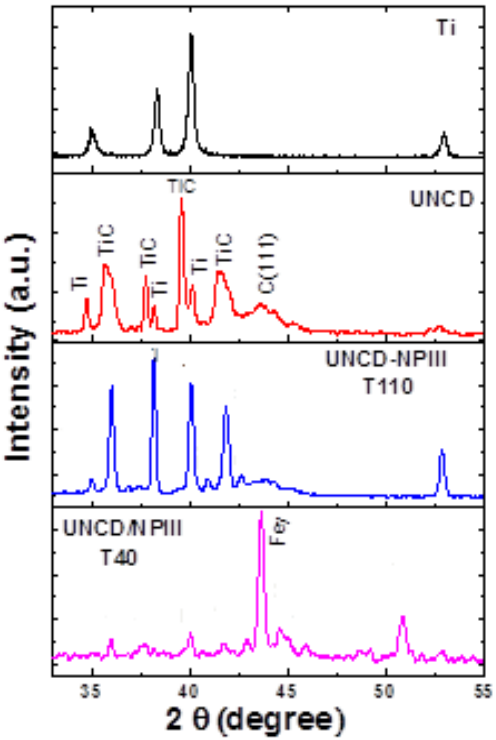

From Fig. 2, it can also be found that for the UNCD films before NPIII treatment, the typical carbon (111) diffraction plane relative to the peak at 44° appears little evidence of low diamond crystallinity. The line broadening of the diamond peak suggests a ballaslike morphology. In addition, apart from the carbon peaks, the most usual TiC formation is clear, related to (111), (200), (220), and (311) planes. The XRD of UNCD films after NPIII treatment in T110 tube contains peaks that correspond to α-Fe (110), (200), and (211) planes (JCPDS No. 06-0696) as resulted from the metal nanoparticles by sputter deposition. It can be seen then that the TiC peaks have disappeared and new peaks have emerged as nitride phase. One can verify the presence of the peaks (111), (200), (220) and (311) for thin TiN film of NaCl-like structure (cubic face centered), with the N atoms replacing the carbon atoms. The XRD pattern of the UNCD film after NPIII in T40 tube contains peaks that correspond to α-Fe and ϒ-Fe that are relatively strong due to intense sputter deposition from the SS304 tube. UNCD film with metal nanoparticles implantation was obtained, which

gives it new prospective applications. However, no diffraction peaks relative to diamond is present anymore in this sample. Therefore, it suggests the presence of high defect density induced by the NPIII, in the case of small diameter tube, providing higher intensity sputter deposition of the metal nanoparticles and higher temperature (780°C).

3.2 FIELD EMISSION GUN SCANNING ELECTRON MICROSCOPY (FEG-SEM) WITH AUXILIARY ENERGY DISPERSIVE SPECTROSCOPY (EDS)

Surface morphologies and EDS analysis of the UNCD film before and after NPIII treatments in T110 and T40 tubes, analyzed by FEG-SEM, are shown in Fig. 3. It can be seen from images, that whilst the UNCD film shows evidence of low crystallinity at this length scale. From the top-view SEM images of the UNCD film before and after NPIII treatment in T110 tube, it can be observed that the structures are similar, as shown in Fig. 3(a) and 3(b). The films presented extremely fine-grained coalescent crystallites, uniformly distributed on the surface of the Ti substrate and abrupt grain boundaries, presenting non-columnar growth structure of a ballaslike morphology. The grains tend to form agglomerates that become more pronounced than those formed after NPIII treatment in T110 tube. These agglomerate sizes are in the range of 42 and 48 nm of diameter, showing grains with an undefined texture for this image magnification. Yang et al. observed the cauliflower or ball-shaped diamond formation, the so-called CVD balls diamond, for argon concentrations above 30%v [19]. They discussed that balls diamond is nearly a pure diamond with strongly twinned microstructure that grows at the transition from faceted diamond to graphite depositions. This morphology is clearly observed in these images. In Fig. 3(b), the UNCD film after NPIII treatment in T110 tube present an appreciable decrease in the carbon concentration and the simultaneous implantation of the nitrogen, oxygen and deposition of metallic nanoparticles such as Fe, Cr and Ni derivation of the stainless steel tube. In Fig. 3(c), the UNCD film after NPIII treatment in T40 tube shows that one-dimensional wire structures are uniformly distributed on the surface of the sample and no diamond structure is seen on the surface. It was estimated that the Fe content in the UNCD is around 73.0 wt% by EDS. It was because of the presence of these Fe atoms, that the UNCD film became magnetic. These results are a consequence of the high temperature (780°C) in smaller diameter tubes used during the NPIII treatment that significantly affect the properties of the UNCD films and it is very important in the transformation process from UNCD film to diamond/metals composite.

Fig. 3. FEG-SEM images and EDS analysis of (a) UNCD films deposited on titanium substrate, (b) UNCD fims treated by NPIII in T110 and (c) UNCD fims treated by NPIII in T40.

(a)

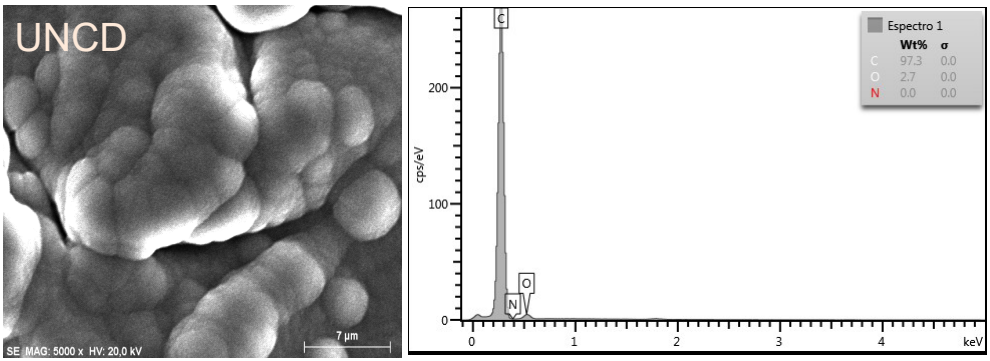

(b)

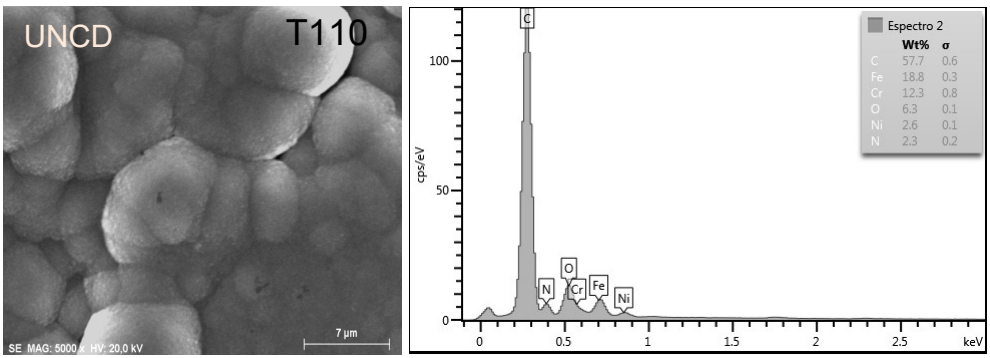

(c)

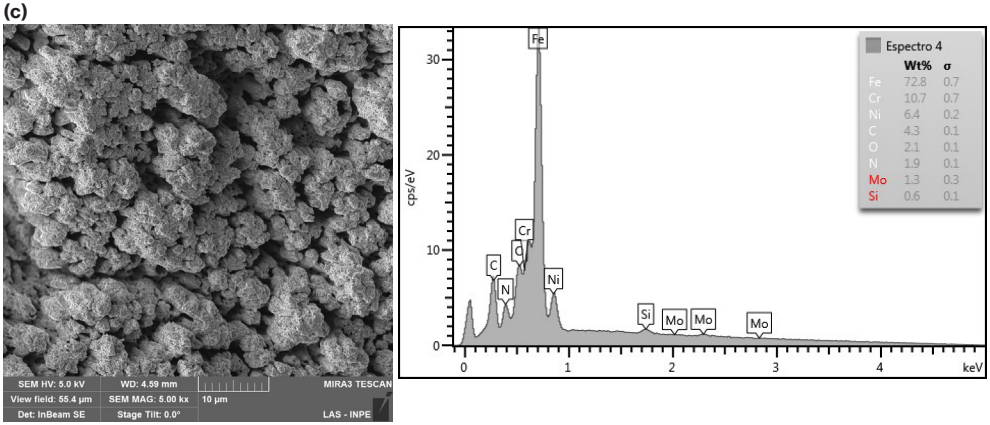

Other elements (Si and Mo) shown in Fig. 3(c) are probably from surface contamination. Based on these results, it is evident that both types of NPIII treatments of the UNCD film result in a very intense surface enrichment of high purity metal

nanoparticles in the surface layer by sputter deposition of these metallic species of the stainless steel coming from the conductive tube. The metal nanoparticles in both cases are characterized by a transfer of electron charge from metallic tube used for the NPIII treatment, which is more pronounced in the case of the T40 tube.

3.3 RAMAN SCATTERING SPECTROSCOPY (RSS)

Raman spectroscopy was used to examine the property of UNCD films before and after NPIII treatments in conductive tubes. Figure 4 shows the measured Raman spectra of the UNCD film before and after NPIII treatment in T110 tube, exhibiting broad bands (D and G) located at approximately 1358 cm^{-1} and 1570 cm^{-1}, which is probably due to surface graphitic structure. G band presence is relative to crystalline graphite impurities and D band represents the presence of disordered graphite. The peak at ~1150 cm^{-1} which is observed in our visible Raman spectra, is attributed as transpolyacetylene segments at the grain boundaries [22] and commonly assigned as to the vibrations of C sp^3 atoms for the UNCD film. Recent works argue that the 1150 cm^{-1} band is due to a deformation mode of the CHx bonds present in the diamond nanoparticles, which showed that an increase of C–H bonds was associated with decreasing in the C–C bonds in the morphology transition from faceted to ballaslike diamond. This conclusion also agrees with theoretical diamond studies proposing that CHx species have a more important role in the growth environment of ballaslike UNCD compared to faceted diamond films [20].

In the second-order Raman spectra, it is possible to observe the band at 2500 to 3500 cm^{-1} attributed to transpolyacetylene (TPA). The TPA (poly-CHx) is as alternate chain of sp^2 carbon atoms, with a single hydrogen bonded to each carbon atom. It is interesting to note that the intensity of this band decreases in the UNCD film after NPIII treatment in T110. The decrease in the intensity of these bands is accompanied by a frequency shift, as can be seen in Table II. This table shows the results of the positions, area, width (FWHM- full width at half-maximum), height and integrated intensity ratio of the D and G bands (I_D/I_G). ID/IG is proportional to the presence of 'disordered' carbon and inversely proportional to graphite crystal size. This is because both the electron and energy transfer mechanisms could result in the reduction of the absorption intensity of the UNCD film after NPIII treatment in T110 tube. The morphologic changes observed by SEM/EDS analysis are also reflected on the Raman spectra features. The evidence of nitrogen and metal nanoparticles incorporations was taken due to great decrease in the intensity of the peaks D and G, besides a pronounced enlargement accompanied with a shift to lower wavenumbers. The intensity of the UNCD film peaks after NPIII treatment in T110 tube

greatly decreased, accompanied with a much wider peak. Due to the fact that metallic ions are heavier in mass, when the implanted Fe ions sit in the diamond lattice (whether the one replace the carbon atom or relax in interstitial sites in diamond lattice), it will introduce strain in the UNCD films. Hence, the strain in the UNCD film after NPIII treatment and the decreasing of the intensity indicate clearly that the structure was changed.

Fig. 4. Raman spectra of UNCD film before and after NPIII treatment in T110 and T40 tubes. The figures inset demonstrate the fitting Raman spectra of the samples.

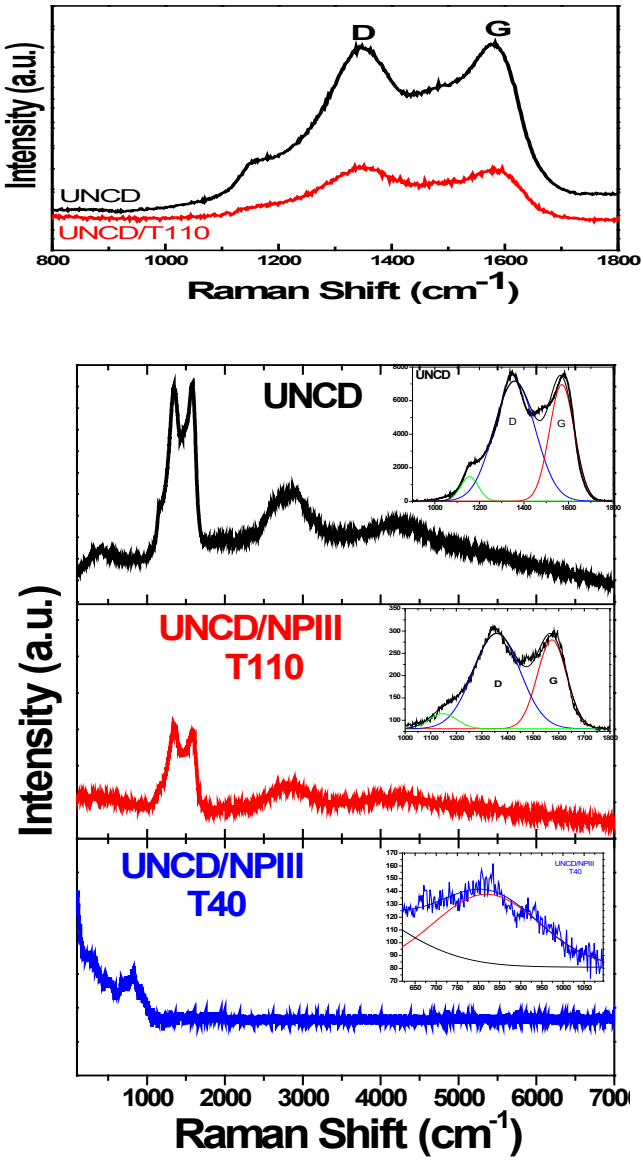

Table II. Position, area, width, height and ID/IG ratio of UNCD film and UNCD film treated by NPIII in T110 and T40 tubes.

514 nm		Position (cm^{-1})	Area ($x10^3$)	Width (cm^{-1})	Height	ID/IG
UNCD		1155.8	146.3	80.0	1458.5	1.03
	D	1358.0	165.4	184.5	7153.5	
	G	1570.1	967.7	111.2	6946.6	
NPIII T110		1147.4	4.65	109.7	33.8	1.07
	D	1357.5	49.1	183.4	213.7	
	G	1573.5	28.5	114.28	199.3	
NPIII T40		818.6	17.8	249.4	56.9	

For UNCD film after NPIII treatment in T40 tube, the structure D and G spectral line is not observed in the Raman shift, suggesting that there is formation of film without carbon phase, which evidently covered the entire surface of the sample. NPIII changed significantly the surface morphologies and characteristics of the Raman peaks. It is a consequence of high concentration of nitrogen implanted into the sample, due to an increase of temperature and to the high ion flux bombardment on the surface, which resulted from an increase of plasma density. One Raman-active broader and asymmetric band at the lower frequency side was observed at about 820 cm^{-1}. It was attributed to the stretching mode vibrations of heavy ions. Metal oxides do not always occur in a crystalline form. When in an amorphous state, the Raman bands are quite broad. The assumption is that in the amorphous form, there is a distortion of interatomic bond angles. Long-range order is lost, but nearest neighbor interactions are affected to shift a particular vibrational frequency. This happens because there is a population of such distortions, and the observed band was broad (width ~250 cm^{-1}), as can be seen in table II. There is often an interest in engineering materials of particular dimensions, especially in nanotechnology. When the dimensions of crystals get small enough, the phonons experience “quantum confinement”. UNCD films can be composed with additional metals, especially chromium, which has the benefit of “passivating” the surface. The Raman bands of the amorphous, supported surface oxide species sharpen and simultaneously shift in frequency at elevated temperatures due to the high ion flux bombardment of nitrogen. High amount of heavy ions sputter deposited from conductive tubes during NPIII treatment of the films. Thus, ion irradiation may be able to alter the surfaces of UNCD films. Several works have been developed in the study of Raman spectroscopy conduted on different UNCD materials with nitrogen in the gas during the synthesis, including studies by Vlasov, Arenal, Ikeda et al [21-23], but the present work is pioneer in the treatement of UNCD films in conductive tubes by NPIII with metal nanoparticle sputter deposition. Thus, the amount or size of the metal nanoparticles supported on the substrates could be appropriately controlled by NPIII parameters.

3.4 X-RAY PHOTOELECTRON SPECTROSCOPY (XPS) ANALYSIS

Until here, we have shown and discussed the morphology and structure of the film and their modifications performed by NPIII. However, there are other important points related to NPIII to take into account, as the atomic configuration and quantification of the nitrogen atoms and metal nanoparticle in the surface. Several groups measured for instance the sp2 and sp3 ratio in UNCD films for the investigation of the CxNx phases, and in order to elucidate the nitrogen bonding environments, have employed XPS technique [24, 25]. Fig. 5 show the XPS wide-large spectra of the UNCD films before and after NPIII treatment in T110 and T40 tubes, and atomic concentration of their components, after 45 minutes etching time. XPS analysis revealed the presence of C (70.63 at%) and O (28.8 at%) in UNCD film as produced.

Fig. 5. XPS wide-scan spectra of the UNCD film before and after NPIII treatment in T110 and T40 tubes.

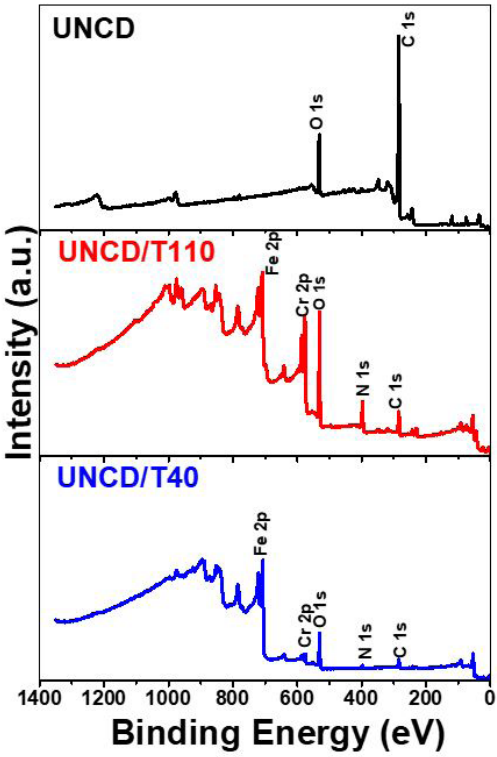

The spectra for UNCD films, after NPIII treatment in T110 and T40 tubes, showed similar characteristic confirming the nitrogen incorporation and metal nanoparticle sputter deposition. However, elemental composition was been significantly changed. UNCD films treated in T110 tube presented high atomic concentration of Fe 2p (49.17 at%) and Cr 2p (34.92at%). These metal elements are typically involved in the formation of a chromium-

rich passive layer on the top surface. UNCD film after NPIII treatment in T40 tube had more of the iron-rich metallic layer relative to Fe 2p (86.10 at%) region.

Fig. 6 shows the high-resolution XPS spectra of UNCD films before and after NPIII treatment in conductive tubes. In Fig. 6(a), the XPS C 1s spectrum of UNCD film before NPIII treatment was deconvoluted to four components with the binding energies of 284.5 eV, 285.3 eV, 287.5 eV, and 288.8 eV. The first component is assigned to the unoccupied π^* bond, which is characteristic of the sp^2 C=C bond (14.12 at%). The second component is due to σ^* bond, which is characteristic of the C-C bond for carbon tetrahedral sp^3 (74.67 at%). The components with higher binding energy, observed between the π^* and σ^* bonds, are characteristic of C-H bond (2.73 at%), and carboxyl group C=O (8.49 at%), respectively. These bonds originate from the absorption of hydrocarbon to the dangling bonds at grain boundaries and oxygen residual gas during the film deposition process [26, 27]. For UNCD film after NPIII treatment in T110 tube (UNCD/T110), one can see that, the component with higher binding energy (288.1 eV) is characteristic of C=N (16.80 at%), and the peak with smaller binding energy (283.3 eV) can be assigned to Fe-C and/or Cr-C bonds (6.42 at%). These peaks are features mainly originating from the nitrogen incorporation and metal nanoparticle sputter deposition from T110. The other two peaks indicate the increase of the amount of sp^2 C=C bond (32.42 at%) and the decrease of C-C bond for carbon tetrahedral sp^3 (44.35 at%). The presence of lower intensity C1s peak implies the increasing of the formation and disorderness of sp^2-bonded carbon phase as a result of the incorporation of nitrogen into UNCD film that have also been-illustrated in Raman spectra (Fig. 4). Another important aspect is the reduction of crystallinity and the increasing of graphitization of the UNCD/T110.

For UNCD film treated in T40 tube, the amounts of sp^2 C=C bond (65.28 at%) and C-metal (12.83 at%) are increased as compared to the UNCD film treated in T110 tube, as can be seen in Fig. 6 (a). The peaks at 288.6 eV and 286.3 eV indicates the amount of the C=O (7.38 at%) and C-O (14.51 at%) bonding in the surface.

In Fig 6 (b), the corresponding N1S band shows asymmetry and involves at least three peaks near 396.9 eV, 397.8 eV, and 398.0 eV for the UNCD film treated in T110 tube. They indicate CrN (34.13 at%), FeN (19.89 at%), and C-Nx (45.98) bonds, respectively. However, in the UNCD films treated in T40 tube, two peaks near 397.1 eV and 398.1eV are present for N 1s band, that correspond to FeN (33.94at%) and C-Nx (66.06 at%) bonds, respectively. The Fe $2p_{3/2}$ peak included four components, whose peaks were centered at 707.1 eV, 708.3 eV, 710.4 eV, and 711.3 eV, as shown in Fig. 6(c). In line with the existing literature [28], we can associate these components with FexN, Fe_3C, Fe_3O_4 and FeOOH phases, respectively. NPIII favored the attainment of an interface type layer consisting of oxide, nitride, metals, sp^2 phases and the diffusion zone characterized by a decreasing C content.

For the UNCD film treated in T40 tube, the peak-to-peak separation (spin-orbital splitting) between these peaks is 13.2 eV, which corresponds to iron metal, as shown in Fig. 6(c). No peak shift was observed in the Fe 2p spectrum but only a decrease in peak intensity due to the sputter deposition layer. Another effect of NPIII in T40 tube that can be emphasized here is the disappearance of the diamond carbon at about 285.3 eV (Fig. 6(a)), which indicates that most of the constituents on the surface are formed by metal nanoparticles sputter deposition from the conductive tube.

Fig. 6. High resolution XPS spectra of (a) C 1s, (b) N 1s, (c) Fe 2p for the UNCD films after NPIII treatment in T110 and T40 tubes.

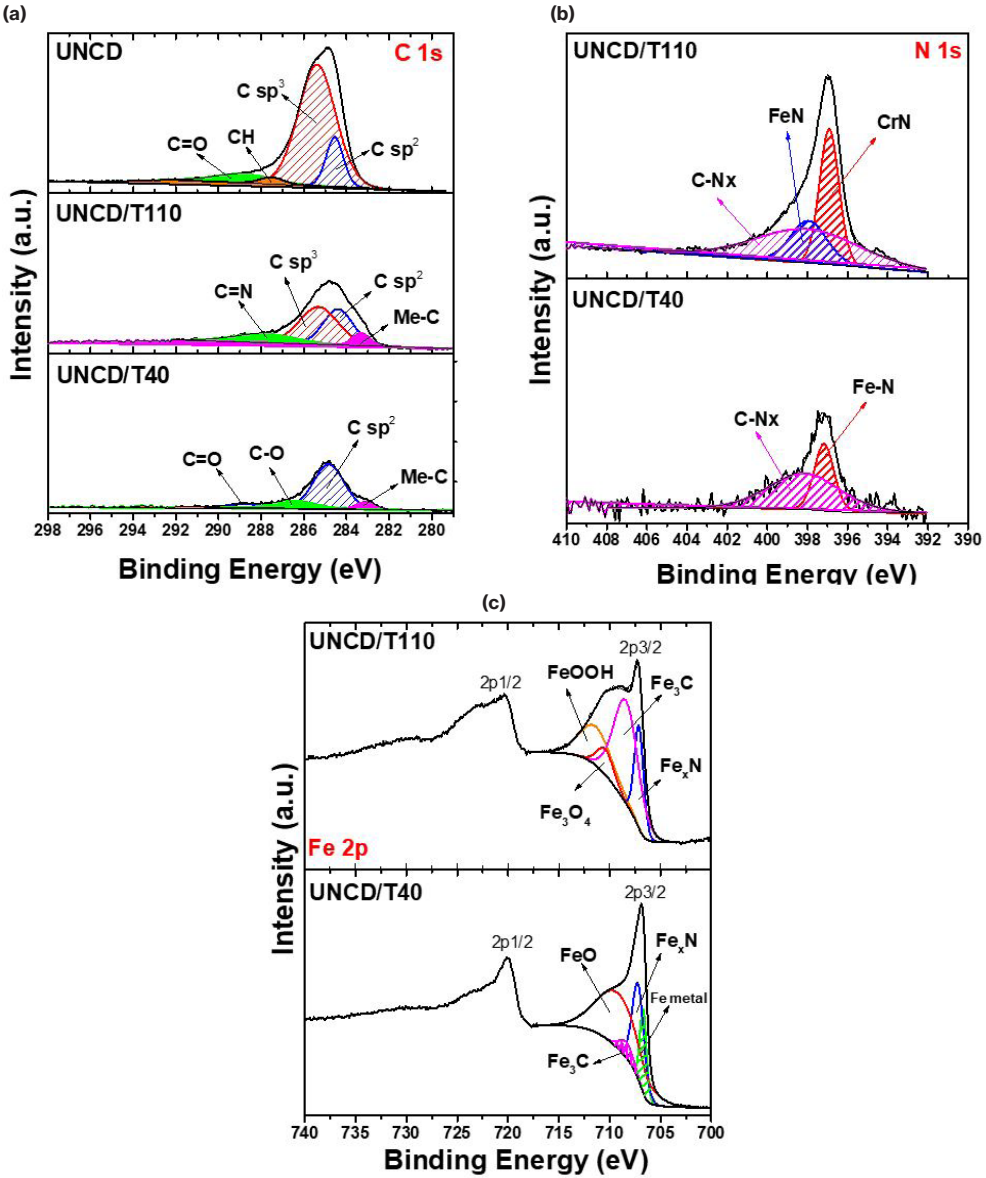

The incorporation of metallic atoms in these UNCD films is capable of creating surface changes and leaving the chemical inertia. This represents a viable path for a number of new applications. The special properties of the diamond for its hardness, thermal conductivity, optical transparency over a wide range of wavelength and chemical stability can be allied to these new features.

4 CONCLUSIONS

The surface modification of UNCD films by NPIII treatments changed the surface morphologies, increased the degree of disorder and the structural defects. In UNCD films after NPIII treatments in T40 tube, diamond and other carbon phases are extinguished on the surface. Analysis of the treated surfaces have demonstrated a substantial dependence of NPIII performance with the tube diameter. Characteristic peaks of metal nanoparticles were found to coexist in the UNCD film after NPIII treatment in T110 tube and it is predominant in samples after NPIII treatment T40 tube case. Raman spectra from the treated samples presented a decrease of the G and D peaks intensities attributed to increase of disorder induced by NPIII/T110 on sp^2 phase (C=N) in the treated UNCD films. EDS results revealed the presence of nitrogen adsorbed in samples and new elements such as metal nanoparticles (Fe, Cr and Ni) by sputter deposition from conductive tube walls. This is a consequence of high concentration of nitrogen implanted into samples, proving the efficiency of the PIII process inside conductive tubes. The results indicate a significant difference of PIII performance when diameter of the tube is reduced from 110 mm to 40 mm. In the case of T40 tube, changes caused by the increase of temperature due to the high ion flux bombarding on the surface, favored larger metal sputter deposition. A strong magnetic field attracted the samples of UNCD films after NPIII treatments in T40 tube. This was an indirect diagnostic feature, which has been used to confirm the magnetic properties of the new film. This was due to the presence of the Fe atoms that can create magnetic carbon structures that could be very useful for protective-coating technology and other nano-electronic device applications. Here we have summarized the key experimental results and the understanding of UNCD films treated in conductive tubes. We have presented an overview of the changes in the properties upon nitrogen incorporation in these films. Applications for these types of new structures have been pointed out.

5 ACKNOWLEDGEMENTS

This research program was supported by Brazilian agencies MCTI and CNPq (Proc. 30008/2015-7/PCI-DA). The authors thank National Nanotechnology Laboratory of Brazil, CNPEN/LNNano/MCTI under proposal XPS-20577.

REFERENCES

[1] Maitz, M. F.; Shevchenko, N. Plasma immersion ion implanted nitinol surface with depressed nickel concentration for implants in blond. Journal of Biomedical Materials Research, v. 76 A, p. 356-365, 2005.

[2] S.F.M. Mariano, M. Ueda, R.M. Oliveira, E.J.D.M. Pillaca, N.M. Santos, Magnetic-field enhanced plasma immersion ion implantation and deposition (PIII&D) of diamond-like carbon films inside tubes, Surface and Coatings Technology 312 (25) (2017) 47-54.

[3] S. Muhl, A. Pérez, Thin Solid Films 579 (2015) 174.

[4] A. Anders, Handbook of Plasma Immersion Ion Implantation & Deposition, John Willey&Sons, New York, 2000.

[5] N. Kumar, K. Panda, S. Dash, J.P. Reithmaier, B.K. Panigrahi, A.K. Tyagi and B. Raj, "Tribological properties of nanocrystalline diamond films deposited by hot filament chemical vapor deposition" AIP Adv., vol. 2, pp. 032164-032156, 2012.

[6] Mello, C. B.; Ueda, M.; Silva, M. M.; Reuther, H.; Pichon, L.; Lepienski, C. M. Tribological effects of plasma immersion ion implantation heating treatments on Ti-6Al-4V alloy. Wear, v. 267, p. 867-873, 2009.

[7] S. Srinivasan, J. Hiller, B. kabius, O. Auciello, Appl. Phys. Let. 90 (2007) 134, 101.

[8] A. V. Sumant, A. R. Kraus, D.M. Gruen, O. Auciello, A. Erdemir, M. Williams, A.F. Artiles, W. Adams, Tribol. Trans. 48 (2005) 24.

[9] P. Bajaj, D. Akin, A. Cupta, D. Sherman, B. Shi, O. Auciello, R. Bashir, Biomed. Microdevices 9 (2007) 787.

[10] O.A. Williams, Semicond. Sci. Technol. 21 (2006) R49.

[11] A.R. krauss, O. Audello, M.Q.Ding, D.M. Gruen, Y. Huang, V.V. Zhirnov, E.I. Givazirzov, A. Breskin, R. Chechen, E. Shefer, V. Konov, S. Pimenov, A. Karabutov, A. Rakhimov, N. Suetin, J. Appl. Phys, 89 (2001) 2958.

[12] S. Bhattacharyya, O. Audello, j. Birrel, J.A. Carlisle, I.A. Curtiss, A.N. Goyette, D.M. Gruen, A.R. Krauss, J. Schlueter, A. Sumant, p. Zapol, Appl. Phys. Lett. 79 (2001) 1441.

[13] O.A. Williams, S. curat, J.E. gerbi, D.M.Gruen, R.B. Jackman, Appl. Phys. Lett. 85 (2004) 1680.

[14] J.M. Blakely, Introduction to the Properties of Crystal Surfaces (Pergamon, Oxford, 1973).

[15] G. Tauber and H.J. Grabke, Ber. Bunsenges. Phys. Chem. 82 (1978) 198.

[16] H. Erhart and H.J. Grabke, Scripta Met. 15 (1981) 531.

[17] J. Robertson, Diamond-like amorphous carbon, materials Science and Engineering R37 (2002) 129-281.

[18] N.M. SANTOS, M. R. V. LANZA, N.G. FERREIRA, M. R. BALDAN, Boron-doped diamond electrodes for carbofuran electrochemical degradation. Bras. Apl. Vác. 35 (2016) 17-24. doi: 10.17563/rbav.v35i1.1002

[19] D.C. Barbosa, M.R. Baldan, V.J. Trava-Airoldi, E.J. Corat, Activation energies for the growth of diamond films and the renucleation of diamond grains during film growth, J. Vac.Sci. Technol.B32 (2014) 3. http://dx.doi.org/10.1116/1.4874308

[20] M. Ueda, A.R. Silva, E.J.D.M. Pillaca, S.F.M. Mariano, R.M. Oliveira, J.O. Rossi, C.M. Lepienski, L. Pichon, New method of plasma immersion ion implantation and also deposition of industrial components using tubular fixture and plasma generated inside the tube by high voltage pulses, Review of Scientific Instruments 87 (2016) 013902. doi: 10.1063/1.4939013

[21] Joint Committee on Powder Diffraction Standards (JCPDS)-International Center for Diffraction Data, Joint Committee on Powder Diffraction Standards Card, 89-5009 (2002).

[22] R. Pfeiffer, H. Kuzmany, p. Knoll, s. Blkova, N. Salk, B. Gunther, evidence for trans-polyacetylene in nano-crystalline diamaond films, Diamond relat. Mater. 12 (2003) 268.

[23] Vlasov I. I., Ralchenko V. G., Goovaerts E., Saveliev A. V. & Kanzyuba M. V. Bulk and surface-enhanced Raman spectroscopy of nitrogen-doped ultrananocrystalline diamond films. Phys Stat Sol (a) 203, 3028–35 (2006).

[24] R. Arenal, P. Bruno, D. J. Miller, M. Bleuel, J. Lai and D. M. Gruen, Phys. Rev. B: Condens. Matter Mater. Phys. 2007,75, 195431

[25] Ikeda, K. Teii, C. Casiraghi, J. Robertson and A. C. Ferrari,J. Appl. Phys., 2008,104, 073720.

[26] K.L. Ma, J.X. tang, Y.S. Zou, Q.Ye, W.J. Zhang, S.T. Lee. Photoemission spectroscopic study of nitrogen incorporated nanocrystalline diamond films, Appl. Physic. Lett. 90 (2007) 092105.

[27] C.C. Teng, S.M. Song, C.M. Sung, C.T. Lin, Structural transformation upon nitrogen doping of ultrananocrystalline diamanod films by microwave plasma CVD, J. Nanomater. 621208, 7 (2009).

[28] L. Ponsonnet, C. Donnet, K. Varlot, J. M. Martin, A. Grill, and V. Patel,Thin Solid Films 319, 97 (1998).

[29] D. S. Grierson, A. V. Sumant, A. R. Konicek, M. Abrecht, J. Birrell, O.Auciello, J. A. Carlisle, T. W. Scharf, M. T. Dugger, P. U. P. A. Gilbert,and R. W. Carpick, J. Vac. Sci. Technol. B 25, 1700 (2007).

[30] J.F. Moulder, W.F. Stickle, P.E. Sobol, K.D. Bomben, Handbook of X-ray Photoelectron Spectroscopy, Perkin-Elmer Corporation, Physical Electronics Division, Eden Prairie (1992).

[31] O.A. Shenderova, D.M. Gruen, Ultrananocrystalline Diamond: Syntheses, Properties, and Applications, William Andrew, chapter 4, p. 125 (2012).

ABOUT THE ORGANIZER

MARCOS AUGUSTO DE LIMA NOBRE: Assistant Professor and Researcher (2006 - present), with citation name M. A. L. Nobre, at the São Paulo State University (UNESP), School of Science and Technology, Department of Physics, campus at Presidente Prudente-SP. Head and Founder (2002) of the Laboratory of Functional Composites and Ceramics (LaCCeF acronym in Portuguese, the native idiom), Lab certified by PROPE-UNESP/National Council for Scientific and Technological Development/CNPq*. Grants from National Council for Scientific and Technological Development (CNPq), 2020-2023, 2019-2021 and 2010-2012. Granted with Young-Researcher scholarship by the São Paulo Research Foundation, FAPESP (São Paulo, São Paulo) (2002 - Summer of 2005). Postdoctoral fellow at the Polytechnic School of the University of Sao Paulo (POLI USP-SP) Metallurgy and Materials Science Department with FAPESP Scholarship (1999-summer of 2000). PhD in Science, CAPES Scholarship (Physical Chemistry 1999) by the Chemistry Department, UFSCar-SP. Master in Chemistry CNPq scholarship (Physical Chemistry 1995) by the Chemistry Department, UFSCar-SP. Licentiate degree (4-year of study) in Physics (1993) CNPq and CNPq-Rhae scholarships by the Physics Department, UFSCar-SP. Associate Editor of the Micro & Nano Letters - IET 2019-2020. Associate Editor of the Micro & Nano Letters-Wiley, 2020 - present. Ethycal Editor of the Applied Mathematics Science (Reuse) m-Hikari and Modern Research in Catalysis, Irvine-CA, USA (2017- date). Editorial board member of the Artemis Editora, Brazil. Nowadays, have 02 patents. Has published 80 papers at 39 different indexed Journals of renowned Editors. In May/25/2021, has been cited 1379 times, at 76 papers (47 with citations), in according to the ResearchID actual Publons base having an H-index equal to 23. Academic Google score: H = 28, i10 = 45 and 2338 citations. Reviewer of more than three dozen of journals. Have more than 580 communications and presentation in National and International Congress and Symposiums, from these 150 has been published as Conference Paper. Author or co-author of 20 Chapters of book approaching Scientific Divulgation, Teaching of Physic and Chemistry for teachers actuating in the graduating degree. For this, the Nanoscience and Nanotechnology have been the first strategy. Received tens of National and International Awards, Honorable mentions and distinction mentions, as well as titles. Research skills: Materials Science, Advanced Ceramic Processing, Linear and Non-linear Advanced Dielectrics Materials, Solid state chemistry, Impedance spectroscopy of solids and fluids, Structural Characterization via Mid infrared Spectroscopy with Fast-Fourier-Transformed of solid and fluids, Structural and non-structural Phase Transitions in Semiconductor Ferroelectrics. Also, Molecular Interactions in Functional Fluids as biofuels and its blends, probed via mid infrared Spectroscopy. Research interests: New Functional Materials as

amorphous composite based on carbon/nanoparticles and Semiconductor Ferroelectrics. Member of the Program of Post-Graduation in Chemistry at UNESP - Campus of São José do Rio Preto, IBILCE UNESP – SP, Brazil.

INDEX

G

K

M

N

O

Z

EDITORA
ARTEMIS